7-2006

An Sveir Model for Assessing Potential Impact of an Imperfect Anti-SARS Vaccine

Abba B. Gumel
University of Manitoba

C. Connell McCluskey
Wilfrid Laurier University, cmccluskey@wlu.ca

James Watmough
University of New Brunswick

MATHEMATICAL BIOSCIENCES
AND ENGINEERING
Volume **3**, Number **3**, July **2006**

http://www.mbejournal.org/

pp. **485–512**

AN SVEIR MODEL FOR ASSESSING POTENTIAL IMPACT OF AN IMPERFECT ANTI-SARS VACCINE

A. B. Gumel

Department of Mathematics, University of Manitoba,
Winnipeg, MB R3T 2N2, Canada.

C. Connell McCluskey

Department of Mathematics, Wilfrid Laurier University,
Waterloo, Ontario, N2L 3C5, Canada.

James Watmough

Department of Mathematics and Statistics, University of New Brunswick,
Fredericton, New Brunswick, E3B 5A3, Canada.

Abstract. The control of severe acute respiratory syndrome (SARS), a fatal contagious viral disease that spread to over 32 countries in 2003, was based on quarantine of latently infected individuals and isolation of individuals with clinical symptoms of SARS. Owing to the recent ongoing clinical trials of some candidate anti-SARS vaccines, this study aims to assess, *via* mathematical modelling, the potential impact of a SARS vaccine, assumed to be imperfect, in curtailing future outbreaks. A relatively simple deterministic model is designed for this purpose. It is shown, using Lyapunov function theory and the theory of compound matrices, that the dynamics of the model are determined by a certain threshold quantity known as the *control reproduction number* ($\mathcal{R}_v$). If $\mathcal{R}_v \leq 1$, the disease will be eliminated from the community; whereas an epidemic occurs if $\mathcal{R}_v > 1$. This study further shows that an imperfect SARS vaccine with infection-blocking efficacy is always beneficial in reducing disease spread within the community, although its overall impact increases with increasing efficacy and coverage. In particular, it is shown that the fraction of individuals vaccinated at steady-state and vaccine efficacy play equal roles in reducing disease burden, and the vaccine must have efficacy of at least 75% to lead to effective control of SARS (assuming $\mathcal{R}_0 = 4$). Numerical simulations are used to explore the severity of outbreaks when $\mathcal{R}_v > 1$.

1. **Introduction.** The World Health Organization (WHO) reported the emergence of a new respiratory disease known as severe acute respiratory syndrome (SARS) in March 2003. The disease, caused by a coronavirus [14, 33, 43], spread rapidly across Asia, Europe and North America, with the highest prevalence in Asia. SARS resulted in about 900 deaths and 8,000 infections globally [30].

SARS was predominantly transmitted from person-to-person *via* close contact. The diagnosis of a probable case was based on clinical symptoms such as fever, dry cough and dyspnea often accompanied by radiographic features of pneumonia [27, 41, 46] and exposure to a source of SARS-CoV [50, 51]. The incubation period

2000 *Mathematics Subject Classification.* 92D30.

Key words and phrases. disease transmission model, vaccination, epidemiology, severe acute respiratory syndrome (SARS), control reproduction number.

for SARS was three to seventeen days, and most infected individuals recover after two to four weeks of illness [7, 15]. The disease nevertheless inflicts a high rate of mortality ($\approx 15\%$), especially among the elderly ($\approx 50\%$) (See [7, 27, 41, 46, 50]).

Owing to the rapid transmissibility of the virus and the fear of a large epidemic, the WHO spearheaded an international effort to combat the spread of SARS. Absent a definitive anti-SARS treatment or vaccine, these efforts were based on the quarantine of suspected cases and isolation of individuals infected with SARS-CoV to stop them from infecting others. Many advances have been made towards the design of a vaccine for SARS, and some vaccines are undergoing clinical trials (see [10, 39, 44, 45, 52, 53]). This is a welcome development since, historically, vaccines have been and continue to be very useful in preventing illness or death of millions of individuals (see, for instance, [40]). However, like almost all other human vaccines, any future SARS vaccine is expected to be imperfect. Such imperfections are defined in terms of numerous characteristics, including a waning immunity or a failure to completely protect all immunized individuals against infection (i.e., the vaccine would allow "breakthrough infection"). Further details on vaccine characteristics can be found in [6, 16, 37].

The aim of this study is to determine, through mathematical modelling, whether a public health strategy based solely on the use of an imperfect vaccine can lead to the effective control of SARS in a community. For the purpose of this study, "imperfect" vaccine means inability to protect all immunized individuals. Since the observed disease timescale is rather short, it is prudent to assume that a future SARS vaccine will confer immunity (incomplete) that does not wane over the time frame of interest (or timescale of disease dynamics). Although numerous mathematical models have been used to assess the impact of anti-SARS control measures based on quarantine and isolation (see, for instance, [11, 19, 31, 32, 42, 48, 49]), no mathematical study has yet been conducted to determine the potential impact of an anti-SARS vaccine.

Over the past few decades, a large number of simple compartmental mathematical models of the general form SVI or SVIR (where S, V, I and R denote the populations of susceptible, vaccinated, infectious and recovered individuals) have been used in the literature to assess the impact or potential impact of imperfect vaccines for combatting the spread of some human diseases (see, for instance, [1, 3, 4, 6, 16, 17, 18, 20, 24, 25, 26, 35, 37] and the references therein). While in some of these studies (e.g., [3, 6, 16, 17, 37]) the vaccine is only given to people newly recruited into the population, such as newborns (cohort vaccination), in many others (e.g., in [1, 20, 26, 35]), a proportion of susceptible individuals is continuously vaccinated. In other studies, such as Arino et al. [4], both cohort and continuous vaccination are provided. Gandon et al. [17] provided a nice study on some of the epidemiological and evolutionary consequences associated with the use of imperfect vaccines using an SVI model with two infected components (unvaccinated infected and vaccinated infected individuals). Their study, which is based on an imperfect vaccine which may decrease probability of infection and/or may decrease the growth rate of parasites within the host, shows that eradication success depends on the type of vaccine and vaccine coverage used. The model constructed in the current paper is an extension of the standard SVIR models, including a new compartment for the latent class (an essential feature of the SARS transmission dynamics). Our model uses continuous vaccination.

The paper is organized as follows. The model is formulated in Section 2. Basic properties of solutions are established in Section 3. The existence and stability of the disease-free equilibrium are analyzed in Section 4. The existence and stability of endemic equilibrium is established in Section 5. A detailed analytical investigation of the final size of the initial outbreak is provided in Section 6.

2. **Model formulation.** The development of the mathematical model is based on subdividing a given SARS-affected community into five compartments: susceptible, $S(t)$, vaccinated, $V(t)$, asymptomatic, $E(t)$, symptomatic, $I(t)$, and recovered, $R(t)$, individuals. The total population size is $N(t) = S(t)+V(t)+E(t)+I(t)+R(t)$.

The rates of change of the populations in each compartment are represented by the following equations:

$$\frac{dS}{dt} = \Pi - \beta SI - \xi S - \mu S, \tag{1}$$

$$\frac{dV}{dt} = \xi S - (1-\tau)\beta VI - \mu V, \tag{2}$$

$$\frac{dE}{dt} = \beta SI + (1-\tau)\beta VI - \alpha E - \mu E, \tag{3}$$

$$\frac{dI}{dt} = \alpha E - \delta I - dI - \mu I, \tag{4}$$

$$\frac{dR}{dt} = \delta I - \mu R. \tag{5}$$

The flow diagram of the model is depicted in Figure 1. The susceptible population is increased by the net in-flow (recruitment) of individuals into the region, either by birth or immigration (at a constant rate Π) and each subpopulation is decreased by natural death (at a rate μ). Administration of an anti-SARS vaccine moves individuals from the susceptible population to the vaccinated population (at a rate ξ).

Susceptible and vaccinated individuals may acquire infection by contact with a SARS-infected individual. It is assumed that the number of contacts between susceptibles and infectives is proportional to the number of susceptibles and to the number of infectives. A certain fraction of these contacts will result in new infections, and so the rate at which susceptibles become infected is βSI, giving what is called mass action. Many researchers argue that the standard incidence formulation is more appropriate for disease transmission in human populations. However, for observed SARS outbreaks, the total population has remained effectively constant. Our simulations, even in the worst case with no disease control measures in effect, show infection of less than 40% of the population, which even with a 15% mortality would lead to only a 6% drop in the total population. In this case, we expect mass action and standard incidence to give similar results.

Since the vaccine is assumed to be imperfect (that is, it does not offer 100% protection against infection), vaccinated individuals also acquire infection *via* contact with symptomatic individuals. Note that, in this case, the effective contact rate, β, is multiplied by a scaling factor $(1-\tau)$, where $0 \le \tau \le 1$ is the efficacy of the vaccine ($\tau = 1$ represents a vaccine that offers 100% protection against infection, whilst $\tau = 0$ models a vaccine that offers no protection at all). In the absence of definitive medical evidence in favour of asymptomatic transmission of SARS, it is assumed

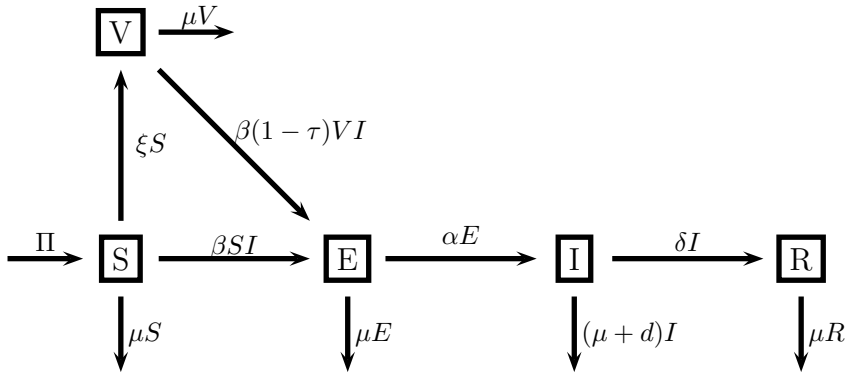

FIGURE 1. Progression of infection from susceptible (S) and vaccinated (V) individuals through the latent (E), infected (I), and treated (R) compartments for the model.

TABLE 1. Parameter values used in the simulations

Parameter	Description	Value
Π	Recruitment rate of susceptible humans	146 *per* day
μ	Natural mortality rate	$1/75$ *per* year $(3.65 \times 10^{-5}$ *per* day)
N_o	Equilibrium population (without disease)	$\Pi/\mu = 4,000,000$
β	Effective contact rate	7.2×10^{-8}*per* day
ξ	Vaccination coverage rate	1 *per* week (0.14 *per* day)
τ	Vaccine efficacy	0.8
α	Rate of development of clinical symptoms	0.125 *per* day
δ	Recovery rate	0.04 *per* day
d	Disease-induced mortality rate	0.008 *per* day

Note: These parameter values give $\mathcal{R}_0 = 6.0$ and $\mathcal{R}_v = 1.2$. The parameters were based on the 2003 SARS outbreak in the Greater Toronto Area. For more details on parameter estimates, see [19].

that only symptomatic SARS-infected individuals (individuals in compartment I) can transmit SARS to susceptible or vaccinated individuals.

Newly-infected individuals (i.e., people in the asymptomatic stage of infection) develop clinical symptoms of SARS (at a rate α). The population in the symptomatic compartment is diminished by recovery (at a rate δ) and disease-induced death (at a rate d).

There is no conclusive evidence in favour or against the notion that SARS infection confers immunity against reinfection. Consequently, it is assumed, in this

study, that recovered individuals do not reacquire SARS infection on the time scale of the epidemic.

It should be mentioned that although the recovered population continues to make contacts with other members of the population, it does not contribute to the transmission dynamics of the disease. Since the recovered population, $R(t)$, does not feature in the first four equations of the model, the rest of the paper will consider only Equations (1)-(4).

3. **Basic properties.** Since the model (1)-(4) monitors populations, it is assumed that $0 \leq \tau \leq 1$ and all other state variables and parameters of the model are nonnegative. It follows that the nonnegative cone, $\mathbb{R}^4_+$, is invariant, as is the disease-free plane ($I = E = 0$).

It is convenient to define $N_o = \dfrac{\Pi}{\mu}$, $S_o = \dfrac{\Pi}{\mu + \xi}$ and $V_o = \dfrac{\xi\Pi}{\mu(\mu + \xi)}$. Notice that we can write $S_o = (1 - p)N_o$ and $V_o = pN_o$ where $p = \xi/(\mu + \xi)$ is the fraction of the population vaccinated at the disease-free equilibrium defined below.

The rate of change of the total population, obtained by adding Equations (1)-(5), is given by

$$\frac{dN}{dt} = \Pi - \mu N - dI \tag{6}$$

with $N = S + V + E + I + R$. It follows that

$$0 < \limsup_{t\to\infty} N(t) \leq N_o,$$

with $\limsup_{t\to\infty} N(t) = N_o$ if and only if $\limsup_{t\to\infty} I(t) = 0$. From Equation (1), it follows that

$$0 \leq \limsup_{t\to\infty} S(t) \leq S_o, \tag{7}$$

and then from Equation (2),

$$0 \leq \limsup_{t\to\infty} V(t) \leq V_o. \tag{8}$$

It follows from Equation (6) that if $N > N_o$, then $\dfrac{dN}{dt} < 0$. This establishes the following lemma.

LEMMA 3.1. *The set*

$$\mathcal{D} = \left\{(S, V, E, I) \in \mathbb{R}^4_+ : S + V + E + I \leq N_o, S \leq S_o, V \leq V_o\right\}$$

is a positively invariant and attracting region for the disease transmission model given by Equations (1)-(4) with initial conditions in $\mathbb{R}^4_+$.

Consequently, in the absence of disease ($I = 0$), the total population, N, approaches the carrying capacity, N_o, asymptotically; and in the presence of disease, the total population is less than or equal to N_o.

Thus, every solution of Equations (1)-(4) with initial conditions in $\mathbb{R}^4_+$ tends toward $\mathcal{D}$ as $t \to \infty$, and every solution with an initial condition in $\mathcal{D}$ remains there for $t > 0$. Therefore, the ω-limit sets of (1)-(4) are contained in $\mathcal{D}$. Furthermore, in $\mathcal{D}$, the usual existence, uniqueness and continuation results hold for the system, so that the system (1)-(4) is well posed mathematically and epidemiologically.

4. The disease-free equilibrium.

4.1. **Existence and local stability of the disease-free equilibrium.** The model given by Equations (1)-(4) has a unique disease-free equilibrium, obtained by setting the right-hand sides of Equations (1)-(4) to zero, given by

$$X_0 = (S_o, V_o, E_o, I_o) = \left(\frac{\Pi}{\xi + \mu}, \frac{\xi \Pi}{\mu(\xi + \mu)}, 0, 0 \right).$$

It can be seen that X_0 attracts the region

$$\mathcal{D}_0 = \{(S, V, E, I) \in \mathcal{D} : E = I = 0\}.$$

To establish the local stability of the disease-free equilibrium, the associated Jacobian of Equations (1)-(4) is evaluated at the disease-free equilibrium. (The Jacobian at a general point is given in (18).) It can be shown that all the eigenvalues of the Jacobian at the disease-free equilibrium have negative real parts if and only if the zeros of the following quadratic are all positive:

$$\lambda^2 + \ (\delta + 2\mu + d + \alpha)\lambda + \ (\alpha + \mu)(\delta + \mu + d)\,(1 - \mathcal{R}_v)\,, \tag{9}$$

where $\mathcal{R}_v$ is defined as

$$\mathcal{R}_v = \frac{\alpha\beta\Pi\,[\mu + (1 - \tau)\xi]}{\mu(\xi + \mu)(\alpha + \mu)(\delta + \mu + d)}.$$

It follows that all zeros of Equation (9) have negative real parts if and only if $\mathcal{R}_v < 1$ (recall that it is assumed that $0 \leq \tau \leq 1$ and all other parameters of the model are nonnegative). Note also that if $\mathcal{R}_v > 1$, then exactly one of the zeros of Equation (9) has positive real part. Thus, we have established the following result:

PROPOSITION 4.1. *The disease-free equilibrium X_0 is locally asymptotically stable if $\mathcal{R}_v < 1$ and unstable if $\mathcal{R}_v > 1$.*

The threshold quantity $\mathcal{R}_v$ is known as the *control reproduction number* of infection. It measures the expected number of new SARS cases generated by an index case (a single infected individual in a completely susceptible population) in a community with a vaccination program in place ($S = S_o$, $V = V_o$). A similar threshold quantity, known as the *basic reproduction number*, is obtained by setting $\xi = 0$ in $\mathcal{R}_v$ giving

$$\mathcal{R}_0 = \frac{\alpha\beta\Pi}{\mu(\alpha + \mu)(\delta + \mu + d)}.$$

The quantity $\mathcal{R}_0$ (see, for instance, [2, 8, 9, 12, 23, 47]) measures the expected number of secondary cases generated by an index case in an unvaccinated, equilibrium population ($S = N_o$, $V = 0$). With this definition for $\mathcal{R}_0$ and introducing

$$p = \frac{V_o}{N_o} = \frac{\xi}{\xi + \mu}$$

as the fraction of the population vaccinated at the disease-free equilibrium we can express $\mathcal{R}_v$ as

$$\mathcal{R}_v = \mathcal{R}_0 \left(\frac{\mu + (1 - \tau)\xi}{\xi + \mu} \right) = \mathcal{R}_0(1 - p\tau). \tag{10}$$

Note that $\mathcal{R}_v \leq \mathcal{R}_0$ with equality only if $\xi = 0$ (ie., $p = 0$) or $\tau = 0$. That is, despite being imperfect, the vaccine (characterized by $\xi > 0$ and $0 < \tau \leq 1$) will allways reduce the reproduction number of the disease. Further arguments and simulations to show that a reduction in $\mathcal{R}_v$ generally implies a reduced and delayed peak caseload, prevalence and disease-induced mortality are summarized in Section 6.

4.2. **Global stability of the disease-free equilibrium.** Biologically speaking, Proposition 4.1 implies that SARS can be eliminated from the SARS-affected region of interest (when $\mathcal{R}_v < 1$) if the initial sizes of the sub-populations of the model are in the basin of attraction of X_0. To ensure that the virus eradication is independent of the initial sizes of the sub-populations of the model, it is imperative to show that the disease-free equilibrium is globally asymptotically stable (GAS). This is done now.

THEOREM 4.1. *The disease-free equilibrium is globally asymptotically stable in* $\mathbb{R}^4_+$ *if* $\mathcal{R}_v \leq 1$.

Proof. Consider the following Lyapunov function:

$$\mathcal{F} = \alpha E + (\alpha + \mu) I \tag{11}$$

with Lyapunov derivative,

$$\begin{aligned}
\mathcal{F}' &= \alpha\Big(\beta\big(S + (1-\tau)V\big)I - (\alpha+\mu)E\Big) + (\alpha+\mu)\big(\alpha E - (\delta + d + \mu)I\big) \\
&= \Big(\alpha\beta\big(S + (1-\tau)V\big) - (\alpha+\mu)(\delta+d+\mu)\Big)I \\
&= (\alpha+\mu)(\delta+d+\mu)\left(\frac{\mathcal{R}_0}{N_o}\big(S + (1-\tau)V\big) - 1\right)I \\
&\leq (\alpha+\mu)(\delta+d+\mu)(\mathcal{R}_v - 1)I \qquad \text{for } (S,V,E,I) \in \mathcal{D}
\end{aligned}$$

by Equations (7) and (8) with equality only at X_0. Since all parameters of the model are nonnegative, it follows that $\mathcal{F}' \leq 0$ for $\mathcal{R}_v \leq 1$ with $\mathcal{F}' = 0$ only if $I = 0$. Hence, $\mathcal{F}$ is a Lyapunov function on $\mathcal{D}$. Further, by Lemma 3.1, $\mathcal{D}$ is a compact, absorbing subset of $\mathbb{R}^4_+$, and the largest compact invariant set in $\{(S,V,E,I) \in \mathcal{D} : \ \mathcal{F}' = 0\}$ is the singleton $\{X_0\}$. Therefore, by the Lasalle invariance principle (see, for instance, [21, Theorem 3.1]), every solution to Equations (1)-(4) with initial conditions in $\mathbb{R}^4_+$ approaches X_0 as $t \to \infty$. □

If $\mathcal{R}_0 < 1$, then the function $\mathcal{F}$ is decreasing whenever $S + (1-\tau)V \leq N_o$. Since $N \geq S + V$, this implies that $\mathcal{F}$ is decreasing if $N \leq N_o$.

4.3. **Implications for disease control.** Theorem 4.1 has important public health implications. It shows that if the imperfect vaccine has sufficient efficacy and coverage rate to make $\mathcal{R}_v \leq 1$, then SARS will be eliminated from the community.

The Lyapunov function (11) shows that the total number of infected individuals $(E + I)$ is a decreasing function of time for $\mathcal{R}_v \leq 1$. However, for $\mathcal{R}_v > 1$, numerical simulations using parameter values relevant to SARS (see [19] for a detailed discussion of parameter values) show that the approach to the endemic equilibrium is not monotonic. Figure 2 shows a simulation of Equations (1)-(4). Populations

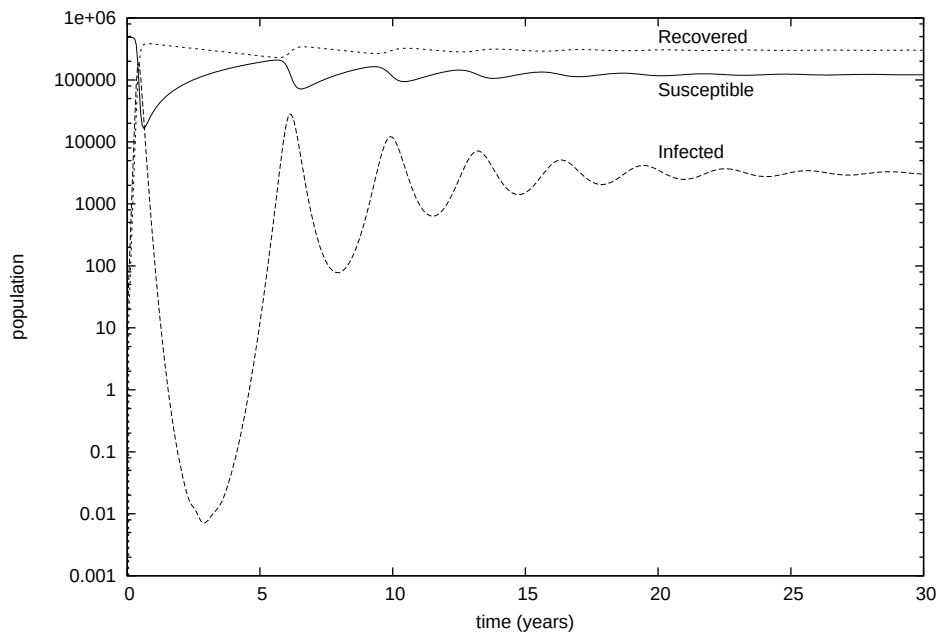

FIGURE 2. Simulation of Equations (1)-(4) showing the oscillatory approach to the endemic equilibrium with no vaccination ($\xi = 0$). The parameters used for the simulation are $\mu = 0.0003$, $\beta = 4.0 \times 10^{-7}$ ($\mathcal{R}_0 = 4$) with the remaining parameters as given in Table 1. These parameters were based on the 2003 SARS outbreak in the Greater Toronto Area. Note the endemic level of infected individuals is 3 136, whereas the initial epidemic peaks at 197 269 infected individuals, a difference of nearly two orders of magnitude. The initial epidemic is shown more clearly in Figure 3.

are shown in a logarithmic scale (base 10). The peak size of the epidemic is several orders of magnitude higher than the final size of the endemic equilibrium. There are two factors that suggest the solutions shown are not realistic. First, the expected number of infected individuals falls well below one during the troughs of the oscillations. This suggests a high likelihood the disease will not persist through the next oscillation. Second, the period of oscillation is several years. We do not expect the assumptions of the model to hold over that timescale: it is reasonable to assume SARS-CoV is seasonal like influenza and other coronaviruses [13], and many factors we have neglected must be taken into account on any longer timescale. Nonetheless, the existence of the endemic solution for $\mathcal{R}_v > 1$ appears to coincide with the epidemic-like transient of the solutions, and the global stability of the disease-free equilibrium for $\mathcal{R}_v \leq 1$ ensures that such epidemics do not occur. Hence, $\mathcal{R}_v$ is a suitable parameter combination with which to gauge the effectiveness of a vaccination program.

Figure 3 shows the populations during the first epidemic. This figure shows the first 250 days of the same simulation run shown in Figure 2. Since the numbers of

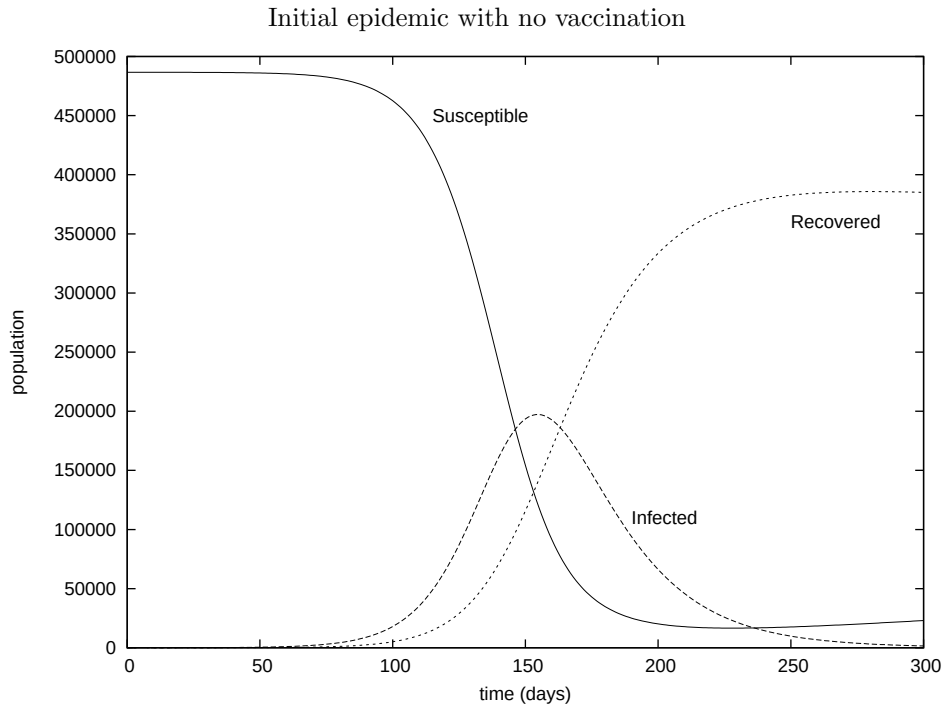

FIGURE 3. Simulation of Equations (1)-(4) showing the initial epidemic with $\xi = 0$ and remaining parameters as per Figure 2. This plot depicts the first 300 days of the simulation in Figure 2.

infected individuals fall to very low levels in the first trough of the oscillations shown in Figure 2, the populations of infected individuals in Figure 3 appear to drop to zero. In fact, the disease-free equilibrium is unstable: the infected population gets close to zero and then slowly grows.

Figure 4 depicts the effectiveness of starting the vaccination program during the initial stages of the epidemic. The simulation is initialized with 10 infectious individuals and the remaining population consisting of unvaccinated susceptibles. This figure must be interpreted with caution: the incidence term in the model is the expected number of new infections per day per infectious individual, and this (deterministic) model ignores variations about that average. While this may be a good approximation when the number of infectious individuals is large, ignoring variations about this average may lead to erroneous results when I is small. In this latter case, a stochastic model is more appropriate. Nevertheless, the predictions of the deterministic model suggest that such a vaccination program would be effective at quickly reducing the control reproduction number and, thereby, bringing the disease under control.

Since $\mathcal{R}_v \leq 1$ is a necessary and sufficient condition for disease elimination (Proposition 4.1 and Theorem 4.1), it follows that the following condition on p is also necessary and sufficient for control:

$$p \geq \frac{1}{\tau}\left(1 - \frac{1}{\mathcal{R}_0}\right) = p_c. \tag{12}$$

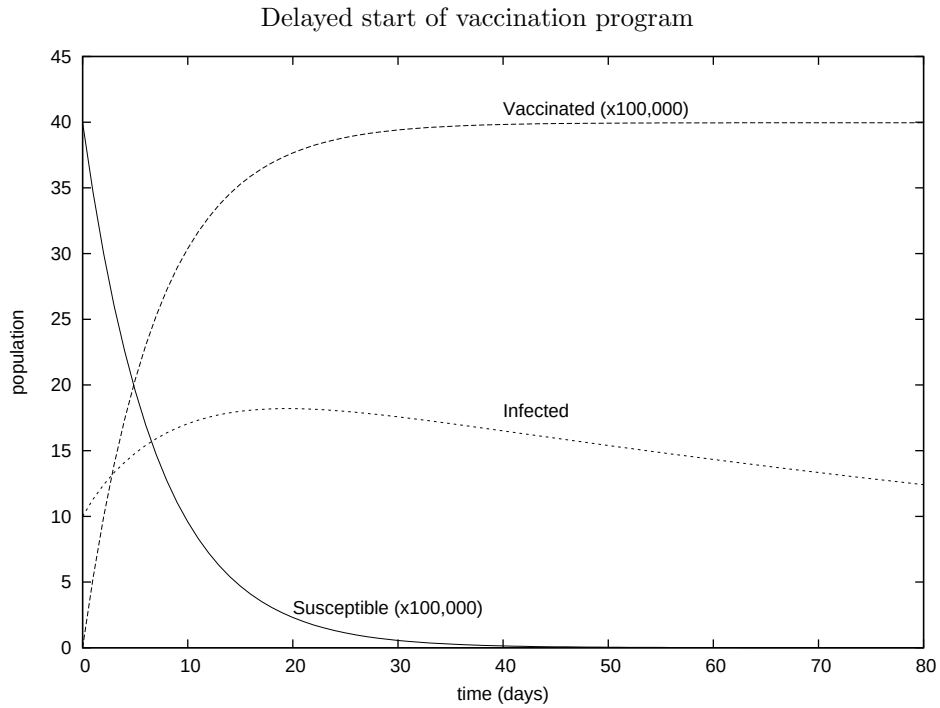

FIGURE 4. Simulation of Equations (1)-(4) showing the initial epidemic with vaccination ($\xi = 1/7$, $\tau = 0.80$, $\beta = 4.8\times10^{-8}$, $\mathcal{R}_0 = 4$, $\mathcal{R}_v = 0.80$, remaining parameters as per Table 1). The susceptible and vaccinated populations are shown in hundred thousands, while the infected population is not scaled.

Proposition 4.1 and Theorem 4.1 can be combined to give the following result:

COROLLARY 4.1. *SARS can be eliminated from the community if* $p \geq p_c$.

Our expression for the threshold vaccinated fraction at equilibrium, p_c, is the same as obtained by Hethcote [22, p. 137]. However, we have shown that this result is still obtained in the case of continuous vaccination and that herd immunity is achieved if the vaccination rate is sufficiently large such that p, the fraction of vaccinated individuals at the disease-free equilibrium, exceeds the critical value p_c.

The critical value, p_c, is plotted as a function of τ for several values of R_o in Figure 5. It is apparent from (10) that both the vaccinated fraction, p, and the vaccine efficacy, τ, play equal roles in reducing $\mathcal{R}_v$ and that both must be high to reduce $\mathcal{R}_v$ below one and thereby control the disease. The inequality (10) can be rewritten as

$$p\tau \geq 1 - \frac{1}{\mathcal{R}_0};$$

it follows that with $\mathcal{R}_0 = 4$, disease control requires the product $p\tau$ exceed 3/4. This region is shown in the upper right of Figure 5. Clearly, for the product to exceed this threshold, both p and τ must be greater than 3/4. In other words, this study shows that if $\mathcal{R}_0 = 4$, then a future SARS vaccine would have to have an

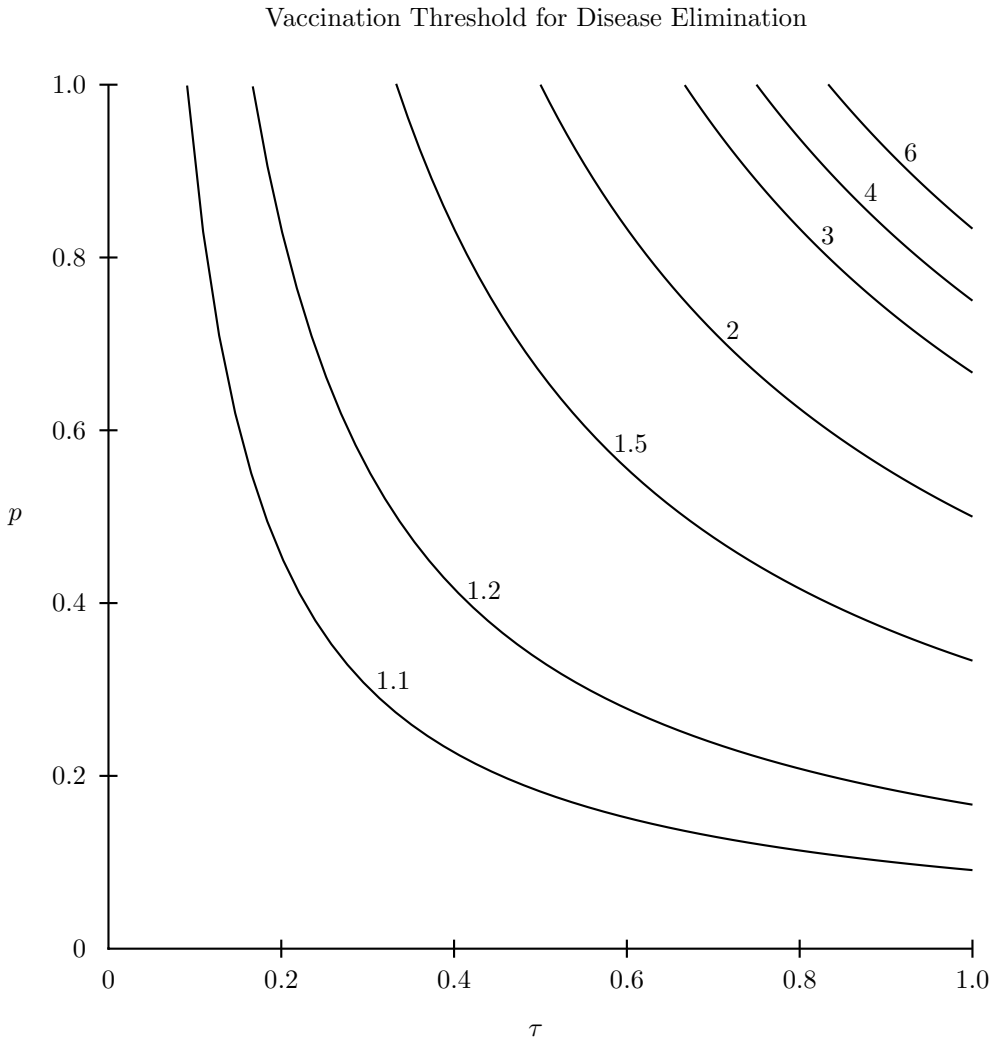

FIGURE 5. Contours obtained from the relation $\mathcal{R}_v = \mathcal{R}_0(1 - p\tau) = 1$ for several values of $\mathcal{R}_0$. For each curve, the region to the above right of the curve consists of the values of p and τ for which the disease-free equilibrium is stable.

efficacy of at least 75% and would have to be administered to at least 75% of the population to eliminate SARS from the community.

The inequality (12) can be expressed in terms of the vaccination rate ξ. This is done by noting, first of all, that the middle expression of Equation (10) is a decreasing function of ξ, and so it is minimized by letting ξ go to infinity. Taking the limit as ξ approaches infinity, we see that this expression is always greater than $(1 - \tau)\mathcal{R}_0$. Thus, if $(1 - \tau)\mathcal{R}_0 \geq 1$, then no amount of vaccination can make $\mathcal{R}_v$

smaller than unity. Alternatively, if $(1-\tau)\mathcal{R}_0 < 1$, then the condition

$$\xi \geq \frac{\mu(\mathcal{R}_0 - 1)}{1-(1-\tau)\mathcal{R}_0} = \xi_c \tag{13}$$

gives $\mathcal{R}_v \leq 1$. Of course, this condition assumes $\mathcal{R}_0 > 1$, since disease elimination follows without vaccination if $\mathcal{R}_0 \leq 1$ (by Proposition 4.1, Theorem 4.1 and the fact that $\mathcal{R}_v \leq \mathcal{R}_0$). It is easy to show, from (13), that $\mathcal{R}_v \leq 1$ if $\xi \geq \xi_c$, and $\mathcal{R}_v > 1$ if $\xi < \xi_c$. Thus, we have established the following result:

PROPOSITION 4.2. *If $(1-\tau)\mathcal{R}_0 < 1$ and $\xi \geq \xi_c$, then SARS will be eliminated from the community. If $(1-\tau)\mathcal{R}_0 \geq 1$, then no amount of vaccination will prevent a SARS outbreak in the community.*

5. **Endemic equilibrium.**

5.1. **Existence of endemic equilibrium.** To find condition(s) for the existence of an equilibrium $X^* = (S^*, V^*, E^*, I^*)$ for which the disease is endemic in the population (i.e. at least one of E^* and I^* is nonzero), Equations (1), (2) and (4) are rearranged to get S^*, V^* and E^* in terms of I^*. This gives

$$S^* = \frac{\Pi}{\beta I^* + \xi + \mu}, \quad V^* = \frac{\xi S^*}{(1-\tau)\beta I^* + \mu}, \quad E^* = \frac{\mu + \delta + d}{\alpha} I^*. \tag{14}$$

Equation (3) yields

$$E^* = \frac{\beta S^* I^* + (1-\tau)\beta I^* V^*}{\alpha + \mu}. \tag{15}$$

Substituting the expressions in Equation (14) into Equation (15), and simplifying, gives the following quadratic in terms of I:

$$P(I) = a_0 I^2 + a_1 I + a_2 = 0 \tag{16}$$

where

$$\begin{aligned} a_0 &= \beta^2(1-\tau), \\ a_1 &= \beta\mu\left(1 + \tfrac{(1-\tau)\mathcal{R}_0}{\mathcal{R}_v}\left(1 - \mathcal{R}_v + (1-\tau)\tfrac{\xi}{\mu}\right)\right), \\ a_2 &= \mu(\xi+\mu)(1-\mathcal{R}_v). \end{aligned} \tag{17}$$

The endemic equilibria of the model are given by Equation (14) with I^* a positive root of Equation (16). Noting that negative endemic equilibria are biologically meaningless, the conditions for $P(I)$ to have positive real roots are determined below.

Suppose $0 \leq \tau < 1$. Then, clearly $a_0 > 0$ and so the quadratic $P(I)$ is concave up. We now do a case analysis to determine the number of positive real zeros of P.

Case 1. Suppose $\mathcal{R}_v > 1$. Then $a_2 < 0$ and so the vertical intercept of $P(I)$ is negative. Combining this with the fact that P is a quadratic which is concave up, it follows that P has two real roots of opposite signs. Thus, the model has a unique positive equilibrium when $\mathcal{R}_v > 1$.

Case 2. Suppose $\mathcal{R}_v = 1$. Then $a_2 = 0$. Here, the quadratic reduces to $P(I) = I(a_0 I + a_1)$, with roots $I^* = 0$ (corresponding to the disease-free equilibrium) and $I^* = -a_1/a_0$. However, it is clear from Equation (17) that $a_1 \geq 0$ for $\mathcal{R}_v = 1$. Thus there is no positive endemic equilibrium for $\mathcal{R}_v = 1$.

Case 3. Suppose $\mathcal{R}_v < 1$. Then $a_0, a_1, a_2 > 0$. Thus, it is clear that there is no positive real root for $\mathcal{R}_v < 1$.

The last case also follows from Theorem 4.1, since global stability of the disease-free equilibrium implies that there are no other equilibria.

The case where $\tau = 1$ is simpler to handle, since $P(I)$ is then linear with $a_0 = 0$ and $a_1 = \beta\mu$. The existence of a positive root of Equation (16) is then reduced to the sign of a_2 being negative, which happens exactly when $\mathcal{R}_v$ is greater than one. We summarize in the following result.

PROPOSITION 5.1. *The model (1)-(4) has a unique positive endemic equilibrium whenever $\mathcal{R}_v > 1$ and no positive endemic equilibrium when $\mathcal{R}_v \leq 1$.*

5.2. **Global stability of the endemic equilibrium.** Proposition 5.1 shows the existence of a unique endemic equilibrium if $\mathcal{R}_v > 1$. We now claim the following (a local stability result for this equilibrium will be given in Section 5.3):

THEOREM 5.1. *For $\mathcal{R}_v > 1$, the unique endemic equilibrium of the model (1)-(4) is globally asymptotically stable in $\mathcal{D} \setminus \mathcal{D}_0$ if $\alpha \leq \mu$.*

Proof. The proof of Theorem 5.1 is based on the method of Li and Muldowney [28, 29]. Let $f = (f_1, f_2, f_3, f_4)^T$, where $f_1,\ f_2,\ f_3$ and f_4 represent the right-hand sides of Equations (1)-(4), respectively. Furthermore, let $x = (S, V, E, I)^T$. Then, the Jacobian matrix for system (1)-(4) is

$$\frac{\partial f}{\partial x} = \begin{bmatrix} -(\beta I + \mu + \xi) & 0 & 0 & -\beta S \\ \xi & -\big((1-\tau)\beta I + \mu\big) & 0 & -(1-\tau)\beta V \\ \beta I & (1-\tau)\beta I & -(\alpha+\mu) & \beta S + (1-\tau)\beta V \\ 0 & 0 & \alpha & -(\delta + d + \mu) \end{bmatrix}. \quad (18)$$

Thus, the second additive compound matrix [38] of the Jacobian matrix is

$$\frac{\partial f}{\partial x}^{[2]} = -\operatorname{diag}\begin{pmatrix} (2-\tau)\beta I + 2\mu + \xi \\ \beta I + 2\mu + \xi + \alpha \\ \beta I + 2\mu + \xi + \delta + d \\ (1-\tau)\beta I + 2\mu + \alpha \\ (1-\tau)\beta I + 2\mu + \delta + d \\ 2\mu + \alpha + \delta + d \end{pmatrix} + \begin{bmatrix} 0 & 0 & -(1-\tau)\beta V & 0 & \beta S & 0 \\ (1-\tau)\beta I & 0 & \beta S + (1-\tau)\beta V & 0 & 0 & \beta S \\ 0 & \alpha & 0 & 0 & 0 & 0 \\ -\beta I & \xi & 0 & 0 & \beta S + (1-\tau)\beta V & (1-\tau)\beta V \\ 0 & 0 & \xi & \alpha & 0 & 0 \\ 0 & 0 & \beta I & 0 & (1-\tau)\beta I & 0 \end{bmatrix}. \quad (19)$$

Let

$$Q = \begin{bmatrix} \frac{1}{E} & 0 & 0 & 0 & 0 & 0 \\ 0 & \frac{1}{E} & 0 & 0 & 0 & 0 \\ 0 & 0 & 0 & \frac{1}{E} & 0 & 0 \\ 0 & 0 & \frac{1}{I} & 0 & 0 & 0 \\ 0 & 0 & 0 & 0 & \frac{1}{I} & 0 \\ 0 & 0 & 0 & 0 & 0 & \frac{1}{I} \end{bmatrix}.$$

Letting $M = Q_f Q^{-1} + Q\frac{\partial f}{\partial x}^{[2]} Q^{-1}$, where Q_f is the derivative of Q in the direction of the vector field f, we see that

$$M = -\begin{pmatrix} (2-\tau)\beta I + \beta\frac{SI}{E} + (1-\tau)\beta\frac{VI}{E} + \mu + \xi - \alpha \\ \beta I + \beta\frac{SI}{E} + (1-\tau)\beta\frac{VI}{E} + \mu + \xi \\ (1-\tau)\beta I + \beta\frac{SI}{E} + (1-\tau)\beta\frac{VI}{E} + \mu \\ \beta I + \alpha\frac{E}{I} + \mu + \xi \\ (1-\tau)\beta I + \alpha\frac{E}{I} + \mu \\ \alpha\frac{E}{I} + \mu + \alpha \end{pmatrix}$$

$$+ \begin{bmatrix} 0 & 0 & 0 & -(1-\tau)\beta\frac{VI}{E} & \beta\frac{SI}{E} & 0 \\ (1-\tau)\beta I & 0 & 0 & \frac{\beta(S+(1-\tau)V)I}{E} & 0 & \beta\frac{SI}{E} \\ -\beta I & \xi & 0 & 0 & \frac{\beta(S+(1-\tau)V)I}{E} & (1-\tau)\beta\frac{VI}{E} \\ 0 & \alpha\frac{E}{I} & 0 & 0 & 0 & 0 \\ 0 & 0 & \alpha\frac{E}{I} & \xi & 0 & 0 \\ 0 & 0 & 0 & \beta I & (1-\tau)\beta I & 0 \end{bmatrix}.$$

We now give a theorem of Li and Muldowney [28], which we will use here to give a condition on the parameters, which when satisfied, implies that the endemic equilibrium is globally asymptotically stable. We reword the theorem for the specific context in which it is being used here. Note that the original theorem [28, Theorem 2.5] involves additional conditions such as $\|Q^{-1}\|$ being bounded, which are satisfied here.

THEOREM 5.2. *If $\mathcal{D}_1$ is a compact absorbing subset of int$(\mathcal{D})$, and there exist $\gamma > 0$ and a Lozinskii measure $\tilde{\mu}$ such that $\tilde{\mu}(M) \leq -\gamma$ for all $x \in \mathcal{D}_1$ then every omega limit point of system (1)-(4) in int$(\mathcal{D})$ is an equilibrium in $\mathcal{D}_1$.*

For $\mathcal{R}_v > 1$, the disease-free equilibrium is repelling towards the interior. In fact, for $\mathcal{R}_v > 1$ there is a compact absorbing set in the interior of $\mathcal{D}$ which attracts all orbits that intersect the interior of $\mathcal{D}$. This gives the following result.

COROLLARY 5.1. *If $\mathcal{R}_v > 1$ and there exists a Lozinskii measure $\tilde{\mu}$ such that $\tilde{\mu}(M) < 0$ for all $x \in int\mathcal{D}$, then each orbit of system (1-4) which intersects $int(\mathcal{D})$ limits to the endemic equilibrium.*

For a norm $\|\cdot\|$ on $\mathbb{R}^n$, the Lozinskii measure $\tilde{\mu}$ associated with $\|\cdot\|$ can be evaluated for an $n \times n$ matrix A as

$$\tilde{\mu}(A) = \inf\{c : \mathcal{D}_+\|z\| \leq c\|z\| \text{ for all solutions of } z' = Az\}, \tag{20}$$

where $\mathcal{D}_+$ is the right-hand derivative [34]. Thus, if we can find a norm on $\mathbb{R}^6$ for which the associated Lozinskii measure satisfies $\tilde{\mu}(M) < 0$ for all $x \in \text{int}\,(\mathcal{D})$ then the endemic equilibrium is globally asymptotically stable for $\mathcal{R}_v > 1$. This has been achieved for a certain subset of the parameter space.

We now define a norm on $\mathbb{R}^6$ for which the definition varies from one orthant to another. Let

$$U_1(z_1, z_2, z_3) = \begin{cases} \max\{|z_1|,\ |z_2| + |z_3|\} & \text{if} \quad \text{sgn}\,(z_1) = \quad \text{sgn}\,(z_2) = \quad \text{sgn}\,(z_3) \\ \max\{|z_2|,\ |z_1| + |z_3|\} & \text{if} \quad \text{sgn}\,(z_1) = \quad \text{sgn}\,(z_2) = -\text{sgn}\,(z_3) \\ \max\{|z_1|,\ |z_2|,\ |z_3|\} & \text{if} \quad \text{sgn}\,(z_1) = -\text{sgn}\,(z_2) = \quad \text{sgn}\,(z_3) \\ \max\{|z_1| + |z_3|,\ |z_2| + |z_3|\} & \text{if} \quad -\text{sgn}\,(z_1) = \quad \text{sgn}\,(z_2) = \quad \text{sgn}\,(z_3) \end{cases}$$

and let

$$U_2(z_4, z_5, z_6) = \begin{cases} |z_4| + |z_5| + |z_6| & \text{if} \quad \text{sgn}\,(z_4) = \quad \text{sgn}\,(z_5) = \quad \text{sgn}\,(z_6) \\ \max\{|z_4| + |z_5|,\ |z_4| + |z_6|\} & \text{if} \quad \text{sgn}\,(z_4) = \quad \text{sgn}\,(z_5) = -\text{sgn}\,(z_6) \\ \max\{|z_5|,\ |z_4| + |z_6|\} & \text{if} \quad \text{sgn}\,(z_4) = -\text{sgn}\,(z_5) = \quad \text{sgn}\,(z_6) \\ \max\{|z_4| + |z_6|,\ |z_5| + |z_6|\} & \text{if} \quad -\text{sgn}\,(z_4) = \quad \text{sgn}\,(z_5) = \quad \text{sgn}\,(z_6). \end{cases}$$

For $z = (z_1, z_2, z_3, z_4, z_5, z_6)^T$, let

$$\|z\| = \max\{U_1, U_2\}.$$

This defines $\|\cdot\|$ on the interior of each orthant. We extend $\|\cdot\|$ continuously to the boundaries of the orthants. One can show that $\|\cdot\|$ is a nonnegative homogeneous function for which the unit ball $\{z : \|z\| \leq 1\}$ is convex and bounded, and so, by Proposition 2.1 of [36], $\|\cdot\|$ is in fact a norm.

We now study solutions to

$$z'(t) = M(t)z(t).$$

Note that the time dependence of $M(t)$ follows from the fact that M depends on S, V, E and I, which in turn depend on t. We now demonstrate that

$$D_+\|z\| < (\alpha - \mu)\|z\|. \tag{21}$$

In a region where $\|z\|$ is a smooth function of z, D_+ is the same as the standard derivative with respect to time. On the other hand, at points for which $\|z\|$ is not smooth (on the coordinate axes, for example), D_+ is still well defined. The full calculation to demonstrate Equation (21) involves sixteen separate cases and subcases, based on the different orthants and the definition of $\|\cdot\|$ within each orthant. We present four representative cases here, including one which gives the most restrictive condition on the parameters. To facilitate the calculations, we note that

$$|z_2|, |z_3|, |z_2 + z_3| \leq U_1(z)$$

and

$$|z_4|, |z_5|, |z_5 + z_6|, |z_4 + z_5 + z_6| \leq U_2(z)$$

for all $z = (z_1, z_2, z_3, z_4, z_5, z_6)^T \in \mathbb{R}^6$.

Case 1. $U_1(z) > U_2(z)$ and $0 < z_1, z_2, z_3$.

Then $\|z\| = \max\{|z_1|, |z_2|+|z_3|\}$. (While the absolute value bars are unnecessary since z_1, z_2, z_3 are positive, they will be important in the later cases. For consistency and to give a clear blueprint for the interested reader to check the omitted cases, we keep the absolute value bars here.)

Case 1A. $|z_1| > |z_2| + |z_3|$.

Then $\|z\| = |z_1| = z_1$ and $U_2(z) < |z_1|$. Taking the right-hand derivative of $\|z\|$, we get

$$\begin{aligned} D_+\|z\| &= z_1' \\ &= \Big(\alpha - (2-\tau)\beta I - \frac{\beta(S + (1-\tau)V)I}{E} - \mu - \xi\Big)z_1 - (1-\tau)\beta\frac{VI}{E}z_4 + \beta\frac{SI}{E}z_5 \\ &\leq \Big(\alpha - (2-\tau)\beta I - \frac{\beta(S + (1-\tau)V)I}{E} - \mu - \xi\Big)|z_1| + (1-\tau)\beta\frac{VI}{E}|z_4| + \beta\frac{SI}{E}|z_5|. \end{aligned}$$

Since $|z_4|, |z_5| \leq U_2(z) < |z_1|$ and $|z_1| = \|z\|$, we have

$$D_+\|z\| \leq \Big(\alpha - (2-\tau)\beta I - \mu - \xi\Big)\|z\|. \tag{22}$$

By linearity, Equation (22) also holds for $U_1 > U_2$ and $z_1, z_2, z_3 < 0$ when $|z_1| > |z_2| + |z_3|$.

Case 1B. $|z_1| < |z_2| + |z_3|$.

Then $\|z\| = |z_2| + |z_3| = z_2 + z_3$ and $U_2(z) < |z_2| + |z_3|$. Taking the right-hand derivative of $\|z\|$, we get

$$\begin{aligned} D_+\|z\| &= z_2' + z_3' \\ &= -\tau\beta I z_1 - \Big(\beta I + \beta\frac{SI}{E} + (1-\tau)\beta\frac{VI}{E} + \mu\Big)z_2 \\ &\quad - \Big((1-\tau)\beta I + \beta\frac{SI}{E} + (1-\tau)\beta\frac{VI}{E} + \mu\Big)z_3 \\ &\quad + \Big(\beta\frac{SI}{E} + (1-\tau)\beta\frac{VI}{E}\Big)\big(z_4 + z_5 + z_6\big) \\ &\leq -\tau\beta I|z_1| - \Big(\beta I + \beta\frac{SI}{E} + (1-\tau)\beta\frac{VI}{E} + \mu\Big)|z_2| \\ &\quad - \Big((1-\tau)\beta I + \beta\frac{SI}{E} + (1-\tau)\beta\frac{VI}{E} + \mu\Big)|z_3| \\ &\quad + \Big(\beta\frac{SI}{E} + (1-\tau)\beta\frac{VI}{E}\Big)|z_4 + z_5 + z_6|. \end{aligned}$$

Since $|z_4 + z_5 + z_6| \leq U_2(z) < |z_2| + |z_3|$ and $-\tau\beta I|z_1| \leq 0$, we have

$$\begin{aligned} D_+\|z\| &\leq -\Big(\beta I + \mu\Big)|z_2| - \Big((1-\tau)\beta I + \mu\Big)|z_3| \\ &\leq -\Big((1-\tau)\beta I + \mu\Big)(|z_2| + |z_3|). \end{aligned}$$

Thus,

$$D_+\|z\| \leq -\Big((1-\tau)\beta I + \mu\Big)\|z\|. \tag{23}$$

By linearity, Equation (23) also holds for $U_1 > U_2$ and $z_1, z_2, z_3 < 0$ when $|z_1| < |z_2| + |z_3|$.

Case 2. $U_1(z) > U_2(z)$ and $z_1 < 0 < z_2, z_3$.
Then $\|z\| = \max\{|z_1| + |z_3|, |z_2| + |z_3|\}$.

Case 2A. $|z_1| > |z_2|$.
Then $\|z\| = |z_1| + |z_3| = -z_1 + z_3$ and $U_2(z) < |z_1| + |z_3|$. Taking the right-hand derivative of $\|z\|$, we get

$$\begin{aligned}
D_+\|z\| &= -z_1' + z_3' \\
&= \Big((1-\tau)\beta I + \beta\frac{SI}{E} + (1-\tau)\beta\frac{VI}{E} + \mu + \xi - \alpha\Big)z_1 + \xi z_2 \\
&\quad - \Big((1-\tau)\beta I + \beta\frac{SI}{E} + (1-\tau)\beta\frac{VI}{E} + \mu\Big)z_3 \\
&\quad + (1-\tau)\beta\frac{VI}{E}\big(z_4 + z_5 + z_6\big) \\
&\leq \Big(\alpha - (1-\tau)\beta I - \beta\frac{SI}{E} - (1-\tau)\beta\frac{VI}{E} - \mu - \xi\Big)|z_1| + \xi|z_2| \\
&\quad - \Big((1-\tau)\beta I + \beta\frac{SI}{E} + (1-\tau)\beta\frac{VI}{E} + \mu\Big)|z_3| \\
&\quad + (1-\tau)\beta\frac{VI}{E}|z_4 + z_5 + z_6|.
\end{aligned}$$

Since $|z_4 + z_5 + z_6| \leq U_2(z) < |z_1| + |z_3|$ and $|z_2| \leq |z_1|$, we have

$$\begin{aligned}
D_+\|z\| \leq \Big(\alpha - (1-\tau)\beta I - \beta\frac{SI}{E} - \mu\Big)|z_1| \\
- \Big((1-\tau)\beta I + \beta\frac{SI}{E} + \mu\Big)|z_3|.
\end{aligned}$$

Recalling that $|z_1| + |z_3| = \|z\|$, yields

$$D_+\|z\| \leq \Big(\alpha - (1-\tau)\beta I - \beta\frac{SI}{E} - \mu\Big)\|z\|. \tag{24}$$

By linearity, Equation (24) also holds for $U_1 > U_2$ and $z_2, z_3 < 0 < z_1$ when $|z_1| > |z_2|$.

Case 2B. $|z_1| < |z_2|$.
Then $\|z\| = |z_2| + |z_3| = z_2 + z_3$ and $U_2(z) < |z_2| + |z_3|$. Taking the right-hand derivative of $\|z\|$, we get

$$\begin{aligned}
D_+\|z\| &= z_2' + z_3' \\
&= -\tau\beta I z_1 - \Big(\beta I + \beta\frac{SI}{E} + (1-\tau)\beta\frac{VI}{E} + \mu\Big) z_2 \\
&\quad - \Big((1-\tau)\beta I + \beta\frac{SI}{E} + (1-\tau)\beta\frac{VI}{E} + \mu\Big) z_3 \\
&\quad + \Big(\beta\frac{SI}{E} + (1-\tau)\beta\frac{VI}{E}\Big)\big(z_4 + z_5 + z_6\big) \\
&\leq \tau\beta I|z_1| - \Big(\beta I + \beta\frac{SI}{E} + (1-\tau)\beta\frac{VI}{E} + \mu\Big)|z_2| \\
&\quad - \Big((1-\tau)\beta I + \beta\frac{SI}{E} + (1-\tau)\beta\frac{VI}{E} + \mu\Big)|z_3| \\
&\quad + \Big(\beta\frac{SI}{E} + (1-\tau)\beta\frac{VI}{E}\Big)|z_4 + z_5 + z_6|.
\end{aligned}$$

Since $|z_4 + z_5 + z_6| \leq U_2(z) < |z_2| + |z_3|$ and $|z_1| \leq |z_2|$, we have

$$D_+\|z\| \leq -\Big((1-\tau)\beta I + \mu\Big)|z_2| - \Big((1-\tau)\beta I + \mu\Big)|z_3|.$$

Thus,

$$D_+\|z\| \leq -\Big((1-\tau)\beta I + \mu\Big)\|z\|. \tag{25}$$

By linearity, Equation (25) also holds for $U_1 > U_2$ and $z_2, z_3 < 0 < z_1$ when $|z_1| < |z_2|$.

Summary of Cases

Combining the results of the four cases presented here in Equations (22)-(25), as well as the remaining twelve cases, we obtain the result

$$D_+\|z\| \leq \max\{-\mu, \alpha - \mu - (1-\tau)\beta I\}\|z\|.$$

Thus, by Equation (20),

$$\tilde{\mu}(M) \leq \max\{-\mu, \alpha - \mu - (1-\tau)\beta I\}.$$

Therefore, if $\alpha \leq \mu$ then $\tilde{\mu}(M) < 0$ on $\operatorname{int}\mathcal{D}$. Thus, Corollary 5.1 implies that for $\mathcal{R}_v > 1$, $\alpha \leq \mu$, the endemic equilibrium is globally asymptotically stable amongst all solutions which intersect the interior of $\mathcal{D}$, completing the proof of Theorem 5.1. □

Theorem 5.1 gives a sufficient condition for the endemic equilibrium to be GAS. In this case, there can be no periodic solutions, homoclinic orbits or heteroclinic cycles. Additionally, extensive numerical simulations suggest that the condition $\alpha \leq \mu$ is not necessary for GAS, but is an artifact of the method. For instance, Figure 2 suggests that the endemic equilibrium is GAS even though α is much larger than μ.

5.3. **Local stability of the endemic equilibrium.** The endemic equilibrium is given by $X^* = (S^*, V^*, E^*, I^*)$. Proposition 5.1 shows the existence of a unique endemic equilibrium if $\mathcal{R}_v > 1$. In Section 5.2, it is demonstrated that if $\mathcal{R}_v > 1$ and $\alpha \leq \mu$, then X^* is globally asymptotically stable (Theorem 5.1), which implies

it is also locally asymptotically stable for $\alpha \leq \mu$. We now show that X^* is locally asymptotically stable whenever it exists (regardless of the values of α and μ).

THEOREM 5.3. *The endemic equilibrium, X^*, is locally asymptotically stable whenever it exists.*

Proof. We first note that the region of parameter space for which $\mathcal{R}_v$ is greater than one is path connected. Thus, any set of parameters for which $\mathcal{R}_v > 1$, can be connected by a path to another set of parameters satisfying $\alpha \leq \mu$, where the entire path satisfies $\mathcal{R}_v > 1$. Thus, X^* is present at each point on the path and is locally asymptotically stable at the endpoint for which $\alpha \leq \mu$. We will now show that while moving along this path there is no loss of stability at X^*.

For the stability of X^* to change when parameters are varied, it is necessary for either a real eigenvalue of $\frac{\partial f}{\partial x}(X^*)$ to pass through zero, or for the real parts of a conjugate pair of complex eigenvalues to pass through zero. In the first case, the determinant of $\frac{\partial f}{\partial x}(X^*)$ is zero at the bifurcation point. In the second case, the sum of the conjugate pair passes through zero. Since the eigenvalues of the second compound of a matrix are the sums of pairs of eigenvalues of the original matrix, the determinant of the second compound of $\frac{\partial f}{\partial x}(X^*)$ must be zero when this second type of bifurcation happens.

Thus, if the determinants of $\frac{\partial f}{\partial x}(X^*)$ and $\frac{\partial f}{\partial x}^{[2]}(X^*)$ are never equal to zero, then X^* never changes stability as parameters are varied. Since the region of the parameter space for which X^* exists is path connected, and X^* is locally asymptotically stable for part of this region (i.e., for $\alpha \leq \mu$), it would follow that X^* is in fact locally asymptotically stable whenever it exists.

Adding the first two rows of $\frac{\partial f}{\partial x}$ as it is given in Equation (18) to the third gives

$$\begin{bmatrix} -(\beta I + \mu + \xi) & 0 & 0 & -\beta S \\ \xi & -\big((1-\tau)\beta I + \mu\big) & 0 & -(1-\tau)\beta V \\ -\mu & -\mu & -(\alpha+\mu) & 0 \\ 0 & 0 & \alpha & -(\delta + d + \mu) \end{bmatrix},$$

which has the same determinant as $\frac{\partial f}{\partial x}$. Expanding along the top row in order to take the determinant gives

$$\begin{aligned} \det\Big(\frac{\partial f}{\partial x}\Big) = {} & \big(\beta I + \mu + \xi\big)\big((1-\tau)\beta I + \mu\big)(\alpha+\mu)(\delta + d + \mu) \\ & - \big(\beta I + \mu + \xi\big)(1-\tau)\beta V \mu\, \alpha \\ & - \beta S\, \xi\, \mu\, \alpha \\ & - \beta S\big((1-\tau)\beta I + \mu\big)\mu\, \alpha. \end{aligned} \tag{26}$$

At X^*, Equation (3) implies $(\alpha+\mu)\frac{E}{I} = \beta S + (1-\tau)\beta V$. Using (4) to replace $\frac{E}{I}$ and multiplying through by α gives

$$(\alpha+\mu)(\delta + d + \mu) = \big(\beta S + (1-\tau)\beta V\big)\alpha.$$

Filling this into the first term on the right-hand side of Equation (26) yields

$$\begin{aligned}\det\Big(\frac{\partial f}{\partial x}(X^*)\Big) &= \big(\beta I+\mu+\xi\big)\big((1-\tau)\beta I+\mu\big)\big(\beta S+(1-\tau)\beta V\big)\alpha\\ &\quad -\big(\beta I+\mu+\xi\big)(1-\tau)\beta V\mu\,\alpha\\ &\quad -\beta S\,\xi\,\mu\,\alpha\\ &\quad -\beta S\big((1-\tau)\beta I+\mu\big)\mu\,\alpha\\ &> 0.\end{aligned}$$

Thus, none of the eigenvalues of $\frac{\partial f}{\partial x}(X^*)$ are ever equal to zero.

Similarly by considering Equation (19) at the endemic equilibrium, it is possible to show

$$\det\Big(\frac{\partial f}{\partial x}^{[2]}(X^*)\Big) > 0.$$

Thus, $\frac{\partial f}{\partial x}(X^*)$ never has a conjugate pair of complex eigenvalues which have real part equal to zero, giving the required result. □

6. **The final size of the initial outbreak.** The size and timing of the peak of the initial epidemic are very sensitive to the vaccination coverage rate and the efficacy of the vaccine. For the parameter values used in Figures 2 and 3, with $\xi = 0$, the epidemic peaks at approximately 115 days and a level near 243,100 infected individuals. When ξ is increased to one per week, the epidemic does not peak until after 3 years and at a level of 7,670 infected individuals (Figure 6). In practice, this would be sufficient to control the disease, since the peak of the outbreak has been delayed beyond the length of a typical disease season.

Figure 7 summarizes the results of 300 simulations of the model. The top two plots show the number of infectious individuals at the peak of the epidemic as a fraction of the initial population (I/N_o) and the lower two plots show the time this peak is reached, in multiples of the mean duration of infection $1/(\mu+d+\delta)$. We see that even if p and τ are insufficient to decrease $\mathcal{R}_v$ below one, the effect of increasing either is to both lower and delay the peak size of the epidemic.

To generate the plots of Figure 7, a rescaled version of the model was used, which had only five independent parameters: $\mathcal{R} = \beta\Pi/\mu/(\mu+d+\delta)$, $\epsilon = \mu/(\mu+d+\delta)$, $\gamma = \alpha/(\mu+d+\delta)$, τ and p. Fifteen sets of the first three parameters were chosen at random (using a Latin hypercube sampling technique [5]) from a uniform distribution: $3 < \mathcal{R} < 6$, $2 < \gamma < 7$ and $0.00026 < \epsilon < 0.0077$. For the plots on the left, p was fixed at 80% and τ was varied between 0 and 1. For the two plots to the right, τ was fixed at 0.8 and p was varied from 0 to 1. The lines in the top figures connect results with identical values for $\mathcal{R}$, c and a.

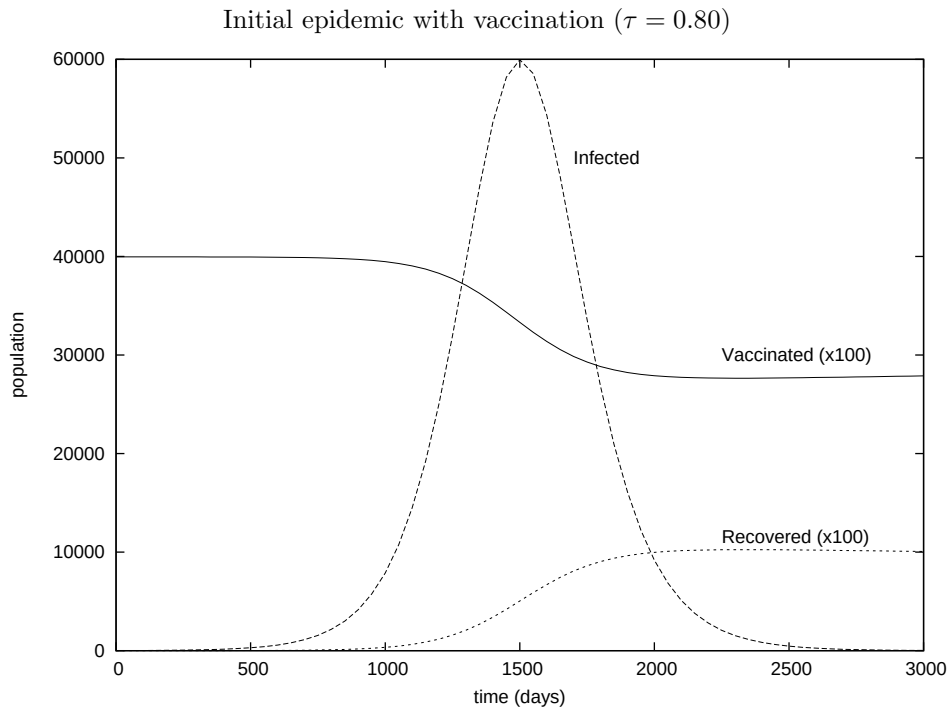

FIGURE 6. Simulation of Equations (1)-(4) showing the initial epidemic with vaccination ($\xi = 0.14$, $\tau = 0.80$, remaining parameters as for Table 1). The vaccinated and recovered populations have been rescaled to fit all curves on the same plot.

To study the initial outbreak in more detail, we rescale the model to match the disease time scale, $1/(d + \delta + \mu)$, and introduce the following rescaled parameters:

$$
\begin{aligned}
N_o &= \frac{\Pi}{\mu}, \\
\epsilon &= \frac{\mu}{(d + \delta + \mu)}, \\
p &= \frac{\xi}{(\xi + \mu)}, \\
\gamma &= \frac{\alpha}{(d + \delta + \mu)}, \\
\beta_o &= \frac{\beta}{(d + \delta + \mu)}.
\end{aligned}
$$

Equations (1) through (4) then become

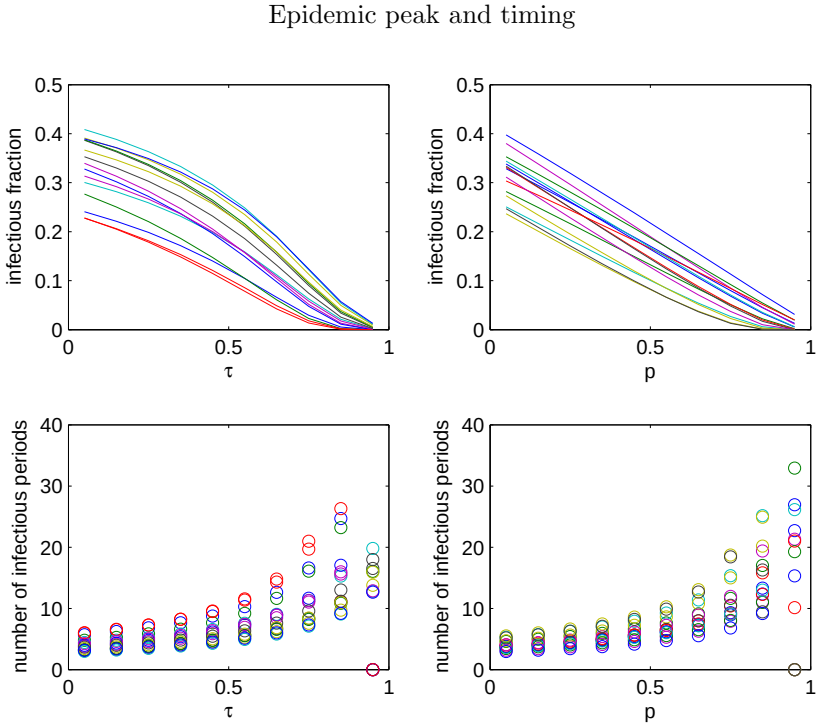

FIGURE 7. These plots summarize 300 simulations of Equations (1)-(4). The upper plots show the fraction of the initial population infectious at the peak of the initial epidemic, and the lower plots show the time taken to reach the peak. The times are given as multiples of the infectious period $1/(\mu + d + \delta)$.

$$\begin{aligned}
\frac{dS}{dt} &= -\beta_o SI + \epsilon\left(N_o - \frac{S}{1-p}\right),\\
\frac{dV}{dt} &= -(1-\tau)\beta_o VI + \epsilon\left(\frac{pS}{1-p} - V\right),\\
\frac{dE}{dt} &= \beta_o\big(S + (1-\tau)V\big)I - (\gamma+\epsilon)E,\\
\frac{dI}{dt} &= \gamma E - (1+\epsilon)I,
\end{aligned}$$

where, for simplicity, t now denotes the rescaled time variable.

For a SARS outbreak in a large community such as the Greater Toronto Area, in Canada, we estimate $\epsilon = 0.00076$, $\beta_o = 0.3$ and $\gamma = 2.6$ [19]. Approximations for the initial peak of solutions to the full model can be obtained by setting $\epsilon = 0$. These approximations are valid until such time as one of the products SI and VI in the first two equations becomes small (comparable in magnitude to the terms involving ϵ). Setting $\epsilon = 0$ gives what we will call the epidemic outbreak model.

$$\frac{dS}{dt} = -\beta_o SI, \tag{27}$$

$$\frac{dV}{dt} = -(1-\tau)\beta_o VI, \tag{28}$$

$$\frac{dE}{dt} = \beta_o\big(S + (1-\tau)V\big)I - \gamma E, \tag{29}$$

$$\frac{dI}{dt} = \gamma E - I. \tag{30}$$

Note that as Π and μ approach zero, with $\Pi/\mu = N_o$, $\mathcal{R}_0$ and $\mathcal{R}_v$ defined previously become

$$\mathcal{R}_0 = \beta_o N_o = \frac{\beta N_o}{d+\delta},$$

and

$$\mathcal{R}_v = \mathcal{R}(S_o) = \mathcal{R}_0(1-p\tau).$$

For the epidemic outbreak model, S and V are nonincreasing functions of time and are decreasing whenever $I > 0$. We also see that the equilibria of the system are all points with $E = I = 0$. Consider a solution with initial conditions corresponding to the disease-free solution of the original model, $S(0) = S_o = (1-p)N_o$ and $V(0) = V_o = pN_o$, and $I(0)$ and $E(0)$ small. From (27) and (28), we see that the solution satisfies

$$\frac{dV}{dS} = \frac{(1-\tau)V}{S}, \qquad V(S_o) = V_o,$$

which can be integrated to obtain V as a function of S:

$$V = V_o\left(\frac{S}{S_o}\right)^{1-\tau}. \tag{31}$$

Defining

$$\mathcal{R}(S) = \beta_o\left(S + (1-\tau)V_o\left(\frac{S}{S_o}\right)^{1-\tau}\right)$$

as the reproduction number during the epidemic, (29) and (30) give

$$\frac{d}{dt}(E+I) = \Big(\mathcal{R}(S) - 1\Big)I. \tag{32}$$

Thus the total infected population, $(E+I)$, is increasing if $\mathcal{R}(S) > 1$ and decreasing if $\mathcal{R}(S) < 1$.

In the previous sections, we examined the stability of the steady state solutions of model (1)-(4). In this section, however, we are interested in the sensitivity of the size of the epidemic to the parameters of the model.

Dividing (32) by (27) yields the relation

$$\frac{d(E+I)}{dS} = \frac{\mathcal{R}(S)-1}{-\beta_o S}, \tag{33}$$

which can be integrated to give

$$E(t) + I(t) = N_o - S(t) - V_o \left(\frac{S(t)}{S_o}\right)^{1-\tau} + \frac{1}{\beta_o} \ln\left(\frac{S(t)}{S_o}\right). \tag{34}$$

Since S and V are decreasing, with $S(0) = S_o$ and $V(0) = V_o$, (34) defines the total infected population, $E + I$, as a function of S with a single maximum when $\mathcal{R}(S) = 1$ and two roots S_1 and S_∞ with $0 < S_\infty < S_1$. Thus, if $\mathcal{R}(S_o) < 1$, $(E + I)$ decreases monotonically to zero and S limits to S_∞. Alternately, if $\mathcal{R}(S_o) > 1$, $(E + I)$ initially increases and then decreases monotonically to zero with S decreasing monotonically from S_o to S_∞. In either case, S_∞ is the final size of the susceptible population.

The fraction of individuals infected over the course of the epidemic is given by

$$1 - \frac{S_\infty + V_\infty}{N_o} = \frac{1}{\mathcal{R}_0} \ln\left(\frac{S_o}{S_\infty}\right), \tag{35}$$

where S_∞ satisfies (34) with $E(t) + I(t) = 0$, $S_o = (1 - p)N_o$, $V_o = pN_o$ and $E_o = I_o = 0$. That is

$$N_o - S_\infty - p\left(\frac{S_\infty}{S_o}\right)^{1-\tau} + \frac{1}{\mathcal{R}_0} \ln\left(\frac{S_\infty}{S_o}\right) = 0.$$

Figure 8 shows how this fraction depends on p, τ and $\mathcal{R}_0$. Vaccines with $\tau < 0.5$ have very little effect on the number of individuals infected, and that the infected fraction is very sensitive to τ. The contour plot is shown for $\mathcal{R}_0 = 4$. The difference in sensitivity for large and small values of τ is even more striking for larger $\mathcal{R}_0$.

7. **Conclusions.** A deterministic model, which incorporates many of the essential epidemiological aspects of SARS-CoV, is designed and used to assess the potential impact of an imperfect SARS vaccine. Some of the main mathematical and biological findings of this study include the following.

(i) The dynamics of the model are almost completely determined by the control reproduction number, $\mathcal{R}_v$. The model has a globally-stable disease-free equilibrium whenever $\mathcal{R}_v \leq 1$, and a unique globally-stable endemic equilibrium whenever $\mathcal{R}_v > 1$ and $\alpha \leq \mu$. This shows that SARS can be eliminated from the community if the imperfect vaccine has sufficient infection-blocking efficacy and coverage rate to bring (and maintain) $\mathcal{R}_v$ to a value less than unity. This result has important public health implications since a vaccination program is presumably more cost-effective than the use of mass quarantine and isolation (which, despite the huge socio-economic burden it inflicts in the community, only results in the detection of a very tiny percentage of infected individuals amongst the large number of quarantined individuals).

(ii) For the SVEIR model considered, an imperfect vaccine is always beneficial to the community, although its overall impact increases with increasing efficacy and coverage rate. This is quite a positive point, since it is known that the use of an imperfect vaccine can sometimes result in detrimental consequences to the community [16, 17]. Many vaccination models [1, 4, 16, 26] possess multiple stable equilibria and exhibit phenomena such as backward and fold bifurcations, where the disease can still persist in the population even when the classical epidemiological requirement of $\mathcal{R}_v < 1$ is satisfied. The features that are thought to lead to these phenomena, in particular waning vaccine

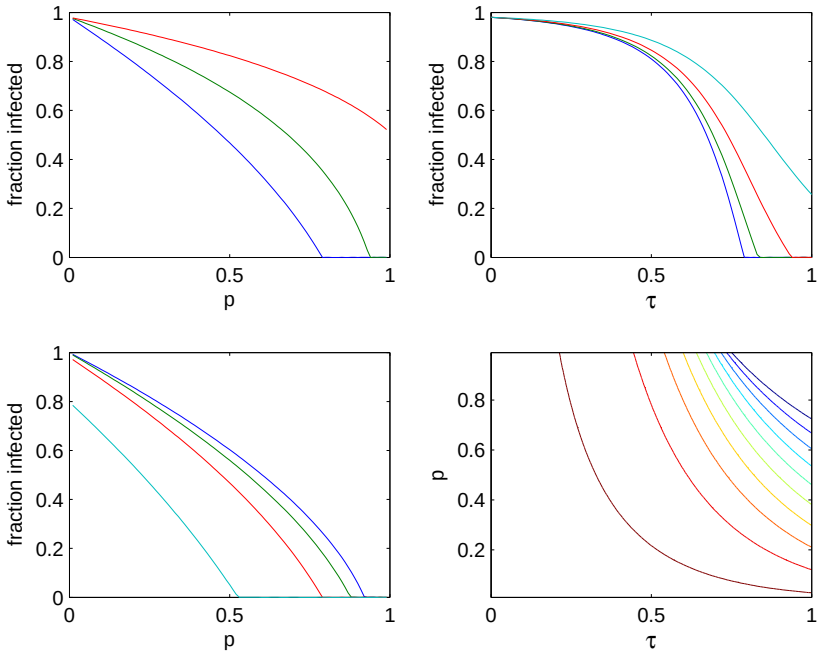

FIGURE 8. Top left: fraction infected, as given by (35), versus p for $\mathcal{R}_0 = 4$ and τ equal to 0.95, 0.80 and 0.65; top right, fraction infected versus τ for $\mathcal{R}_0 = 4$ and p equal to .95, 0.90, 0.80, and 0.60; bottom left: fraction infected versus p for $\tau = 0.95$ and $\mathcal{R}_0$ equal to 2, 4, 6, and 8; bottom right: contour plot of infected fraction versus p and τ, level curves are shown for infected fractions of $0.05, 0.10, \ldots 0.95$.

and recovery without imunity, are assumed to be absent in SARS, or at least not evident at the disease time scale.

(iii) A threshold fraction of individuals to be vaccinated at steady-state (p_c) to attain herd immunity is determined.

(iv) The vaccine efficacy and vaccinated fraction play equal roles in reducing the control reproduction number (and, therefore, disease control), and both must be reasonably high to eliminate the disease.

(v) The vaccine efficacy needs to be at least 75% for effective control of SARS outbreaks if $\mathcal{R}_0 = 4$.

Overall, this study shows that a future SARS vaccine (assumed to be imperfect) that can make the control reproduction number less than unity will effectively control future SARS outbreaks in the community. This vaccine will, however, fail to prevent outbreaks if it cannot make (and keep) the control reproduction number below unity. It should be mentioned that this study is based on a relatively simple model. The model needs to be refined as more further data (and knowledge) becomes available.

Acknowledgements. Research supported in part by MITACS and NSERC discovery grants to JW and ABG.

REFERENCES

[1] Alexander, M. E., Bowman, C., Moghadas, S. M., Summers, R., Gumel, A. B. and Sahai, B. M. (2004). A vaccination model for transmission dynamics of influenza. *SIAM J. Appl. Dyn. Syst.* **3**(4): 503-524.

[2] Anderson, R. M. and May, R. M. (1991). *Infectious Diseases of Humans*, Oxford Univ. Press, London.

[3] Anderson, R. M. and Garnett, G. P. (1996). Low-efficacy HIV vaccines: potential for community-based intervention programmes. *Lancet* **348**: 1010-1013.

[4] Arino, J., McCluskey, C. C., van den Driessche, P. (2003). Global results for an epidemic model with vaccination that exhibits backward bifurcation. *SIAM J. Appl. Math.* **64**(1): 260-276

[5] Blower, S. M. and Dowlatabadi, H. (1994). Sensitivity and uncertainty analysis of complex models of disease transmission: and HIV Model, as an example. *International Statistical Review* 62(2): 229-243.

[6] Blower, S. M. and A. McLean (1994). Prophylactic vaccines, risk behavior change, and the probability of eradicating HIV in San Francisco. *Science* **265**: 1451-1454.

[7] Booth, C. M. (and 20 others) (2003). Clinical features and short-term outcomes of 144 patients with SARS in the Greater Toronto area. *JAMA* **289**: 1-9.

[8] Brauer, F. and Castillo-Chavez, C. (2000). *Mathematical Models in Population Biology and Epidemiology*. Texts in Applied Mathematics Series, Volume 40, Springer-Verlag, New York.

[9] Castillo-Chavez, C., Feng, Z. and Huang, W. (2002). On the computation of $\mathcal{R}_0$ and its role on global stability. Mathematical Approaches for Emerging and Reemerging Infectious Diseases: An Introduction. The IMA Volumes in Mathematics and its Applications. Volume 125, pp. 229-250, Springer, New York. Castillo-Chavez, C. with S. Blower, P. van den Driessche, D. Kirschner and A.-A. Yakubu (Eds.)

[10] China in SARS vaccine trial. The Scientist, January 12, 2004. http://www.biomedcentral.com/news/20040121/03

[11] Chowell, G., Fenimore, P. W., Castillo-Garsow, M.A. and Castillo-Chavez, C. (2003). SARS outbreaks in Ontario, Hong Kong and Singapore: the role of diagnosis and isolation as a control mechanism. *J. Theoret. Biol.* **224**: 1-8.

[12] Diekmann, O. and Heesterbeek, J. A. P. (2000).*Mathematical Epidemiology of Infectious Diseases: Model Building, Analysis and Interpretation*, Wiley, New York.

[13] Dowell, S. F. and Ho, M. S. (2004). Seasonality of infectious diseaseand severe acute respiratory syndrome – what we don't know can hurt us, *Lancet Infect Dis* 4: 704-08

[14] Drosten, C. (and 24 others) (2003). Identification of a novel coronavirus in patients with severe acute respiratory syndrome. *N. Engl. J. Med.* **348**: 1967-1976.

[15] Dwosh, H. A., Hong, H. H., Austgarden, D., Herman, S. and Schabas, R. (2003). Identification and containment of an outbreak of SARS in a community hospital. *CMAJ* **168**: 1415-1420.

[16] Elbasha, E. H. and Gumel, A. B. Theoretical assessment of public health impact of imperfect prophylactic HIV-1 vaccines with therapeutic benefits. *Bulletin of Mathematical Biology*. To appear.

[17] Gandon, S., Mackinnon, M., Nee, S. and Read, A. (2003). Imperfect vaccination: some epidemiological and evolutionary consequences. *Proc. Roy. Soc. Lond., Series B* **270**: 1129-1136.

[18] Glass, K. and Grenfell, B. (2003). Antibody dynamics in childhood diseases: waning and boosting of immunity and the impact of vaccination. *J. Theoret. Biol.* **221**(1): 121-131.

[19] Gumel, A. B., S. Ruan, T. Day, J. Watmough, F. Brauer, P. van den Driessche, D. Gabrielson, C. Bowman, M. E. Alexander, S. Ardal, J. Wu and B. M. Sahai (2004). Modeling strategies for controlling SARS outbreaks based on Toronto, Hong Kong, Singapore and Beijing experience. *Proc. Roy. Soc. Lond.,Series B* **271**: 2223-2232.

[20] Gumel, A. B., Moghadas, S. M. and Mickens, R. E. (2004). Effect of a preventive vaccine on the dynamics of HIV transmission. *Commun. Nonlinear Sci. Numer. Simul.* **9**: 649-659.

[21] Hale, J. K. (1969). Ordinary differential equations, John Wiley & Sons, New York

[22] Hethcote, H. W. (1989). Three basic epidemiological models, in Levin, S.A., Hallam, T.G. & Gross, L.J (eds) Applied Mathematical Ecology, Springer-Verlag, Berlin, pp. 119-144

[23] Hethcote, H. W. (2000). The mathematics of infectious diseases. *SIAM Review* **42**: 599-653.
[24] Hethcote, H. W. (2001). New vaccination strategies for pertussis. Mathematical Approaches for Emerging and Reemerging Infectious Diseases: An Introduction. IMA Series on Mathematics and Its Applications, Springer, New York, **25**: 97-118. C. Castillo-Chavez, S. Blower, P. van den Driessche, and D. Kirschner (eds.).
[25] Hethcote, H. W., Horby, P. and McIntyre, P. (2004). Using computer simulations to compare pertussis vaccination strategies in Australia. *Vaccine* **22**: 2181-2191.
[26] Kribs-Zaleta, C. and Velasco-Hernández, J. (2000). A simple vaccination model with multiple endemic states. *Math. Biosci.* **164**: 183-201.
[27] Ksiazek, T. G. (and 25 others) (2003). A novel coronavirus associated with severe acute respiratory syndrome. *N. Engl. J. Med.* **348**: 1953-1966.
[28] Li, M. Y. and Muldowney, J. S. (1995). On R. A. Smith's autonomous convergence theorem. *Rocky Mount. J. Math.* **25**: 365-379.
[29] Li, M. Y. and Muldowney, J. S. (1996). Phase Asymptotic Semiflows, Poincaré's Condition and the Existence of Stable Limit Cycles. *J. Diff. Eq.* **124**: 425-448.
[30] Lingappa, J. R., McDonald, L. C., Simone, P. and Parashar, U. D. (2004). Wresting SARS from uncertainty. *Emerging Infectious Diseases* **10** No.2: 167-170.
[31] Lipsitch, M. (and 11 others) (2003). Transmission dynamics and control of severe acute respiratory syndrome. *Science* **300**: 1966-1970.
[32] Lloyd-Smith, J. O., Galvani, A. P. and Getz, W. M. (2003). Curtailing transmission of severe acute respiratory syndrome within a community and its hospital, *Proc. Royal Soc. London Series B*, **270**: 1979-1989.
[33] Marra, M. A. (and 57 others) (2003). The genome sequence of the SARS-associated coronavirus. *Science* **300**: 1399-1404.
[34] Martin Jr., R. H. (1974). Logarithmic norms and projections applied to linear differential systems. *J. Math. Anal. Appl.*, **45**: 432-454.
[35] Massad, E., F. Coutinho, M. Burattini, L. Lopez, and C. J. Struchiner (2001). Modeling the impact of imperfect HIV vaccines on the incidence of the infection. *Math. Comput. Modelling* **34**: 345-351.
[36] McCluskey, C. C.. A strategy for constructing Lyapunov functions for non-autonomous linear differential equations. *Linear Algebra and its Applications (to appear).*
[37] McLean, A. and Blower, S. (1993). Imperfect vaccines and herd immunity to HIV. *Proc. Roy. Soc. Lond. B* **253**: 9-13.
[38] Muldowney, J. S. (1990). Compound matrices and ordinary differential equations. *Rocky Mountain J. Math.*, **20**: 857-872.
[39] Pang, H., Liu, Y., Han, X., Xu., Y, Jiang, F., Wu, D., Kong, X., Bartlam, M. and Rao, Z. (2004). Protective humoral responses to severe acute respiratory syndrome-associated coronavirus: implications for the design of an effective protein-based vaccine. *J Gen Virol.* **85**: 3109-13.
[40] Plotkin, S. A. and Orenstein, W. A. (eds) (1999). *Vaccines*, 3rd edn., Philadelphia, PA: W. B. Saunders.
[41] Poutanen, S. M. (and 19 others) (2003). Identification of severe acute respiratory syndrome in Canada. *N. Engl. J. Med.* **348**: 1995-2005.
[42] Riley, S. (and 19 others) (2003). Transmission dynamics of etiological agent of SARS in Hong Kong: the impact of public health interventions. *Science* **300**: 1961-1966.
[43] Rota, P. A. (and 34 others) (2003). Characterization of a novel coronavirus associated with severe acute respiratory syndrome. *Science* **300**: 1394-1399.
[44] Sinovac Biotech Co. (2004). Sinotoc biotech ltd. has received a further US $1.2 million in government research funding for SARS vaccine. See www.sinovac.com/en/content.asp?ID=231.
[45] Tamburri, R. (2004). SARS vaccine undergoing animal testing. *CMAJ* **171**(4): 320.
[46] Tsang, K. W. (and 15 others) (2003). A cluster of cases of severe acute respiratory syndrome in Hong Kong. *N. Engl. J. Med.* **348**: 1977-1985.
[47] van den Driessche, P. and Watmough, J. (2002). Reproduction numbers and sub-threshold endemic equilibria for compartmental models of disease transmission. *Math. Biosci.* **180**: 29-48.
[48] Wang, W. and Ruan, S. (2003). Simulating the SARS outbreak in Beijing with limited data. *J. Theoret. Biol.* **227**: 369-379.

[49] Webb, G. F., Blaser, M. J., Zhu, H., Ardal, S. and Wu, J. (2004). Critical role of nosocomial transmission in the Toronto SARS outbreak. *Mathematical Biosciences and Engineering.* **1**(1): 1-13.
[50] WHO (2003a). Cumulative number of reported probable cases of SARS. See www.who.int/csr/sars/country/en.
[51] WHO (2003b). Case definitions for surveillance of severe acute respiratory syndrome (SARS). See www.who.int/csr/sars/casedefinition/en.
[52] Xiong, S. (and 13 others) (2004). Immunogenicity of SARS inactivated vaccine in BALB/c mice. *Immunol Lett.* **95**(2): 139-143.
[53] Yang, Z., W. Kong, Y. Huang, A. Roberts, B. R. Murphy, K. Subbarao and G. J. Nabel (2004). A DNA vaccine induces SARS coronavirus neutralization and protective immunity in mice. *Nature* **428**: 561-564.

Received on September 13, 2005. Accepted on January 17, 2006.

E-mail address: gumelab@c.umanitoba.ca
E-mail address: ccmcc8@gmail.com
E-mail address: watmough@unb.ca